

Kinetic, Thermodynamic, and Mechanistic Patterns for Free (Unbound) Cytochrome *c* at Au/SAM Junctions: Impact of Electronic Coupling, Hydrostatic Pressure, and Stabilizing/Denaturing Additives

Dimitri E. Khoshtariya,^{*[a, b]} Tina D. Dolidze,^[b] Stefan Seifert,^[c] David Sarauli,^[a] Geoffrey Lee,^[c] and Rudi van Eldik^{*[a]}

Abstract: Combined kinetic (electrochemical) and thermodynamic (calorimetric) investigations were performed for an unbound (intact native-like) cytochrome *c* (CytC) freely diffusing to and from gold electrodes modified by hydroxyl-terminated self-assembled monolayer films (SAMs), under a unique broad range of experimental conditions. Our approach included: 1) fine-tuning of the charge-transfer (CT) distance by using the extended set of Au-deposited hydroxyl-terminated alkanethiol SAMs [-S-(CH₂)_{*n*}-OH] of variable thickness (*n* = 2, 3, 4, 6, 11); 2) application of a high-pressure (up to 150 MPa) kinetic strategy toward the representative Au/SAM/CytC assemblies (*n* = 3, 4, 6); 3) complementary electrochemical and microcalorimetric studies on the impact of some stabilizing and denaturing additives. We report for the first time a mechanistic changeover detected for “free” CytC

by three independent kinetic methods, manifested through 1) the abrupt change in the dependence of the shape of the electron exchange standard rate constant (*k*^o) versus the SAM thickness (resulting in a variation of estimated actual CT range within ca. 15 to 25 Å including ca. 11 Å of an “effective” heme-to-ω-hydroxyl distance). The corresponding values of the electronic coupling matrix element vary within the range from ca. 3 to 0.02 cm⁻¹; 2) the change in activation volume from +6.7 (*n* = 3), to ≈ 0 (*n* = 4), and -5.5 (*n* = 6) cm³ mol⁻¹ (disclosing at *n* = 3 a direct pressure effect on the protein’s internal viscosity); 3) a “full” Kramers-type viscosity dependence for *k*^o at *n* =

2 and 3 (demonstrating control of an intraglobular friction through the external dynamic properties), and its gradual transformation to the viscosity independent (nonadiabatic) regime at *n* = 6 and 11. Multilateral cross-testing of “free” CytC in a native-like, glucose-stabilized and urea-destabilized (molten-globule-like) states revealed novel intrinsic links between local/global structural and functional characteristics. Importantly, our results on the high-pressure and solution-viscosity effects, together with matching literature data, strongly support the concept of “dynamic slaving”, which implies that fluctuations involving “small” solution components control the proteins’ intrinsic dynamics and function in a highly cooperative manner as far as CT processes under adiabatic conditions are concerned.

Keywords: charge-transfer mechanisms • cytochrome *c* • electrochemistry • kinetics • self-assembled monolayers • thermodynamics

Introduction

Despite the modest molecular dimensions and a relatively “simple” function, the mechanistic understanding of cytochrome *c* (CytC) and the whole *c*-type cytochrome family is still far from satisfactory with regard to two most fundamental aspects, namely, molecular recognition and the charge-transfer (CT) functionality.^[1,2] These types of biomolecules, which contain covalently integrated iron–heme moieties as redox centers, are known to shuttle electrons in cellular photosynthetic and/or respiratory systems of living cells.^[1,2] However, the recently disclosed role of CytC in cell apoptosis^[3] may serve as an indication of a much higher functional and mechanistic complexity in this type of protein than was thought before. To the same extent, an obstacle in the clari-

[a] Prof. Dr. D. E. Khoshtariya, Dipl.-Phys. D. Sarauli, Prof. Dr. R. van Eldik
Institute for Inorganic Chemistry
University of Erlangen-Nürnberg, Egerlandstrasse 1
91058 Erlangen (Germany)
Fax: (+49)9131-85-27387
E-mail: dimitri.k@joker.ge
vaneldik@chemie.uni-erlangen.de

[b] Prof. Dr. D. E. Khoshtariya, Dr. T. D. Dolidze
Institute of Molecular Biology and Biophysics
Institute of Inorganic Chemistry and Electrochemistry
Georgian Academy of Sciences, Gotua 12, 0160 Tbilisi (Georgia)
Fax: (+995)32-959-157

[c] Dr. S. Seifert, Prof. Dr. G. Lee
Department of Pharmaceutical Technologies
University of Erlangen-Nürnberg, Cauerstrasse 4
91058 Erlangen (Germany)

fication of cytochrome patterns due to a high diversity of the intermolecular interactions should be mentioned. Indeed, there is much evidence that at least some well-studied cytochromes, including CytC (or its modified variants), operate either in a strongly (irreversibly) bound, loosely bound (almost freely diffusing), or in both of these regimes depending on the specific intracellular (in vivo) or experimental conditions.^[4–10] Furthermore, these diverse interactions may control the proteins' essential properties (including structural, stability, and dynamic characteristics) and, hence, the intrinsic redox mechanisms and their interplay.^[6–10] The latter aspect, in turn, is closely connected with an old puzzle that concerns the thermodynamic stability of globular proteins,^[11–15] as well as a novel problem on the coupling of the proteins' external and internal dynamic properties and their hierarchical inter-relevance ("dynamic slaving").^[16–18] All these issues are synergistically connected and require profound studies by means of complementary cross-testing strategies (e.g., combining kinetic and thermodynamic, and/or different kinetic, namely, high-pressure and solvent viscosity approaches). However, preferably, selection of some reference experimental (environmental) conditions would be rational implying minimization/unification of molecular interactions at the starting point, *vide infra*.

Experimental information on the CT kinetics in liquid-phase systems involving CytC and its native or artificial redox partners (redox proteins, complex ions, etc.) is extensive (see for example, Refs. 19–22). However, even for this well-characterized protein,^[1,2,23a] systematic mechanistic studies in "homogeneous" systems are moreover complicated, owing to restrictions in independent and gradual variation of factors determining both molecular recognition and intrinsic CT patterns. Instead, as an unfortunate prerequisite (unavoidable for cases of traditional solution systems), an extra environmental (structural and dynamic) complexity is introduced by the participating redox partner.^[21,22] The strategy of covalent attachment of "small" complex ions as redox counterparts at different external sites of CytC,^[19,20] although offering significant insights, does not permit sufficiently smooth variation of intrinsic parameters, such as electronic coupling (correlated with the CT distance; see below), due to the highly inhomogeneous nature of the protein interior.^[1,2]

In contrast, the artificial bioelectrochemical devices that are composed of Au-deposited self-assembled monolayer (SAM) films of variable composition and thickness, with redox proteins irreversibly attached or freely diffusing to the SAM terminal groups,^[23–31] seem to be free of the above-mentioned limitations. They offer a number of novel properties that can be classified, on the one hand, as regarding the relevance to intrinsic CT mechanisms implying almost unlimited possibilities of the easy variation of SAMs' chain length (thickness) and their internal composition (by using aliphatic, π -conjugated, or alternating/mixed chains). Both factors greatly affect the electronic coupling strength, thus allowing for a variation of the rate constant over many orders of magnitude,^[24,25,27,29–31] and an eventual mechanistic

changeover that has been indicated for a few bioelectrochemical assemblies,^[30a,b] as well as for a model electrochemical system involving metal complex redox couples.^[29,33] On the other hand, as regarding the molecular recognition mechanisms, the possibility of almost unlimited variation of the SAMs' terminal components (including inert, electrostatically, or specifically active groups), and their mixtures should be mentioned.^[24,28]

The advantages of bioelectrochemical kinetic approaches and subsequent mechanistic analysis were basically captured by systematic kinetic studies for the irreversibly attached CytC regarding the variation of the SAM terminal-group composition (ω -COOH^[24,26,30] vs. ω -Py^[27,29]), along with the variation of SAM thickness ($n=2$ to 21).^[26–30] For the case of freely diffusing CytC, previous work includes the variation of the SAM composition (implying "primitively" organized SAMs of typically small organic molecules with fixed SAM thickness),^[36] variation of the electrode overvoltage (at fixed n),^[25] variation of a denaturant (urea) concentration, mostly at low pH (no systematic variation of n),^[23b] and variation of hydrostatic pressure^[32] (including the first high-pressure (HP) kinetic study of a bioelectrochemical system restricted to "primitive" thin SAMs of invariable n ^[32a]).

However, systematic kinetic studies for free CytC (e.g., diffusing to ω -OH) with essentially variable n , are still lacking. Other pieces also remained fragmentary and did not address some principle inherent links among the structural and functional properties of redox proteins that can be manifested through the correlations between the corresponding kinetic and thermodynamic parameters. Synergistic links between different kinetic approaches (e.g., implying the variations of hydrostatic pressure and solution viscosity) that provide complementary mechanistic information, could also be of great advantage. Taking into account the necessity of further complex and systematic investigations on such a model redox protein as CytC under some "reference" conditions, implying exclusion of the a priori strong (and poorly controllable) alterations by other large-scale items, such as other (partner) protein molecules, phospholipid membranes or SAM arrays, we offer in the present report results of unprecedented extensive mechanistic investigations of CytC covering the following aspects (for a preliminary report on some aspects of the present work, see reference [32b]):

- 1) Systematic bioelectrochemical kinetic studies with the involvement of hydroxyl-terminated alkanethiol SAMs (weakly interacting with CytC) of variable thickness providing variation of the electronic coupling factor within the maximum (measurable in a freely diffusing regime) broad range (with $n=2$ to 11), hence allowing for the hypothetical mechanistic changeover from the adiabatic (strong electronic coupling, thin SAMs) limit to the non-adiabatic (weak electronic coupling, thick SAMs) limit, as was demonstrated earlier for CytC bound to ω -COOH- and ω -Py-terminated SAMs.
- 2) Extension of previous HP bioelectrochemical kinetic studies^[32a] for primitive thin SAMs to the series of simi-

lar devices, involving in this case CytC freely diffusing to ω -OH-terminated SAMs of essentially variable thickness, to test for the first time the CT mechanistic changeover through HP kinetic studies.

- Further extension of these kinetic studies applying variable solution viscosity to free CytC aiming at an additional test of the mechanistic changeover (proven earlier for irreversibly attached CytC). Comparative analysis of the impact of solvent viscosity and HP aimed at new insights into the issue of dynamic slaving.^[17,18b] In addition, testing of the thermodynamic stabilizing effect of a viscous additive, glucose, by differential scanning calorimetry (DSC, vide infra).
- Combining the kinetic (electrochemical fast scan cyclic voltammetric, FSCV) and thermodynamic (DSC) strategies for the rigorous cross-testing of intercorrelated kinetic and thermodynamic manifestations of the glucose-induced, presumably highly stabilized, and urea-induced, presumably partially denatured (molten-globule-like, MG), states all at neutral (physiological) pH.

The FSCV technique^[34,35] was in most cases (for $n=2, 3, 4, 6$) applied to determine the heterogeneous standard rate constant, a method that has been proven to be fully adequate for both the determination of the physical condition (structural accomplishment) of composite self-assembled systems, and accurate determination of dynamic characteristics, such as heterogeneous kinetic constants and diffusion coefficients, under variable experimental conditions.^[32a,33a,36]

Theoretical background: For freely diffusing reactant species, such as CytC, the experimentally determined standard heterogeneous rate constant, k_{het}^0 , within the framework of the conventional encounter pre-equilibrium model, can be written as Equation (1),^[37] in which K_A is a statistically averaged pre-equilibrium term (which normally can be assumed to be constant within the series of SAMs with identical terminal groups, vide infra^[32a,33]), and k_{ET}^0 is the intrinsic unimolecular electron-transfer (ET) rate constant representative of either a nonadiabatic or adiabatic process.

$$k_{\text{het}}^0 = K_A k_{\text{ET}}^0 \quad (1)$$

Theoretical work that accounts for both these mechanisms and the smooth turnover between them is available.^[29b,37c,38–40] The recently updated expression is that given in Equation (2),^[29b] in which H_{if} is the electronic coupling matrix element, λ is the reorganization free energy, and ρ_m is the density of electronic states in the metal (electrode).

$$k_{\text{ET}}^0 = \frac{(H_{\text{if}})^2}{\hbar} \frac{\rho_m}{1+g} \left(\frac{\pi^3 RT}{\lambda} \right)^{1/2} \exp\left(-\frac{\Delta G_a}{RT}\right) \quad (2)$$

The activation free energy is defined by Equation (3),^[41,42] in which ΔG_0 is the free energy gap (throughout the present work $\Delta G_0=0$ by definition of the standard heterogeneous rate constant, see Experimental Section).

$$\Delta G_a = \frac{(\lambda - \Delta G_0)^2}{4\lambda} - H_{\text{if}} \quad (3)$$

The adiabaticity criterion, g , that acts as a control parameter is given by Equation (4),^[29b,38,40] in which the effective frequency ν_{eff} is related to a single or several relaxation process(es) in the vicinity of the reaction zone that are intrinsically coupled to electron transfer (actually, $\nu_{\text{eff}} \sim \eta$, in which η is the medium's effective viscosity).^[38–40]

$$g = \frac{\pi^3 RT (H_{\text{if}})^2 \rho_m}{\hbar \nu_{\text{eff}} \lambda} \quad (4)$$

See also references [43–46] for the first general and later phenomenological formulations. Whether $g \ll 1$ or $g \gg 1$ [depending on the values of the intrinsic parameters from Eq. (4), especially of H_{if} , the value of which can be varied greatly in our experiments], one arrives at two different expressions for the intrinsic rate constant [Eqs. (5) and (6)], with the following phenomenological extensions:

$$k_{\text{ET}} \propto \exp[-\beta(R_e - R_0)] \quad (5)$$

$$k_{\text{ET}} \propto \eta^{-\delta} \quad (6)$$

The expression in Equation (5) is that for long-range CT, in which R_e is the CT distance, R_0 is the distance at minimal reactant–electrode separation, and β is the decay parameter for alkanethiol spacers normally of the order of ca. 1 \AA^{-1} .^[26–30,33] The expression given in Equation (6) is that for the short-range CT, in which δ is an “empirical” solvent–protein coupling parameter with values between 0 and 1, with $\delta \approx 1$ standing for full solvent–protein coupling.^[37–40,44–46]

Prediction of high-pressure kinetic effects: High-pressure (HP) kinetic studies provide unique information about the activation volumes for various processes, adding a new dimension to the development of fundamental mechanistic understanding.^[23,48–50] Application of this technique along (or in combination) with other kinetic approaches seems to be promising with respect to biological processes, including charge-transfer (CT) reactions.^[23,51] A general expression for the activation volume of any kind of microscopic barrier-crossing process, including ET can be defined as,^[37,47–49]

$$\Delta V_a = -RT \left[\frac{\partial(\ln k)}{\partial P} \right]_T \quad (7)$$

After substitution of Equation (2), skipping minor terms, and taking into account Equations (3) and (5) applicable in the nonadiabatic case, one obtains Equation (8) (see also references [50,51]).

$$\Delta V_a(\text{NA}) = \beta RT \left(\frac{\partial R_e}{\partial P} \right)_T + \frac{1}{4} \left(\frac{\partial \lambda}{\partial P} \right)_T \quad (8)$$

Equation (8) indicates that when the pre-equilibrium con-

stant [Eq. (1)] is not affected by pressure (*vide infra*) and the nonadiabatic (long-range tunneling) mechanism [Eq. (5)] is operative, the experimentally measurable volume of activation may originate from the effects of pressure on the ET distance due to shrinking of the reactive (here SAM/protein) system and/or change in the medium (SAM/protein/solvent) reorganization energy (Franck-Condon factor).

If we now consider the effect of pressure on the adiabatic (viscosity-dependent) ET process [Eqs. (4) and (8)] and skipping again the minor terms, it can be written as Equation (9),^[49a,c] from which it follows that in the case of full dynamic (viscosity) control [Eq. (6)], the viscosity changes due to increasing pressure may result in a large positive contribution, provided that viscosity is affected by pressure.

$$\Delta V_a(AD) = RT \left(\frac{\partial \ln \eta}{\partial P} \right)_T + \frac{1}{4} \left(\frac{\partial \lambda}{\partial P} \right)_T \quad (9)$$

This is the case for all known liquids except water (see references [32a,49a,c] and references cited therein). Actually for most solvents, η increases exponentially with pressure, and yields the maximum net viscosity-related contribution as high as +20 cm³ mol⁻¹ (as upper limit,^[49a] see also further discussion).

In addition, we assume that in the case of composite multicomponent systems like in the present case, the overall medium reorganization energy can roughly be reproduced by the summation over individual components [Eq. (10)],^[52,53] in which the three contributions represent the solvent, protein, and SAM interior reorganization (*vide infra*).

$$\lambda = \lambda_{\text{solv}} + \lambda_{\text{prot}} + \lambda_{\text{SAM}} \quad (10)$$

Results and Discussion

Impact of the CT distance (electronic coupling)—new evidence for the mechanistic changeover: Figure 1 illustrates the impact of SAM thickness ($n=3, 6, \text{ and } 11$) on the CV response at a constant CV scan rate, 0.05 V s⁻¹, along with the CV response upon the variation of CV scan rate for ω -OH SAMs of different thickness (for $n=2$ and 6) recorded at the highest pressure applied in this work (see Experimental Section for the description of data processing). Figure 2 represents the logarithmic dependence of the experimental standard heterogeneous rate constant (k_{het}^0) on the number of SAM methylene units (see also Table 1). For clarity, Figure 2 depicts only the data obtained with solutions in 500 mM Tris-HCl buffer (pH 7.4). The data set obtained with solutions in 2 mM phosphate buffer (plus 0.5 M KCl, pH 7.4), did not differ notably from the former one (Table 1). The upper plot, clearly distinguishable for SAMs with $n=2, 3, \text{ and } 4$, represents kinetic data obtained in the absence of a stabilizing viscose additive glucose (and any other special

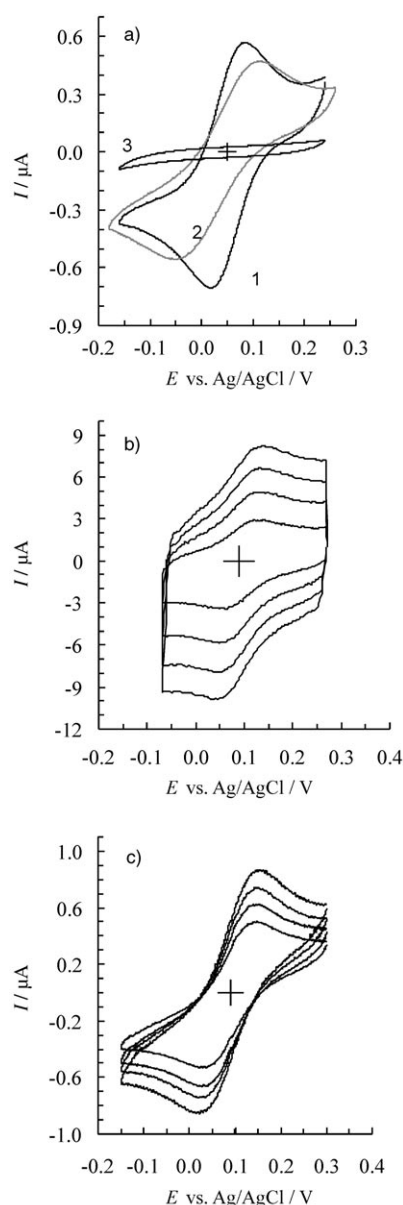


Figure 1. a) CVs for CytC electron exchange at Au electrodes modified by hydroxy-terminated *n*-alkanethiol SAMs of variable thickness. 1): $n=3, 2$); $n=6, 3$); $n=11$. Ambient pressure, scan rate: 0.05 V s⁻¹; b) CVs for CytC electron exchange at Au electrodes modified by hydroxy-terminated *n*-alkanethiol SAM, $n=2$, $P=150$ MPa, scan rates: 1, 2, 3, and 4 V s⁻¹ (peak uprising); c) CVs for CytC electron exchange at Au electrodes modified by hydroxy-terminated *n*-alkanethiol SAM, $n=6$, $P=150$ MPa, scan rates: 0.03, 0.05, 0.07, and 0.1 V s⁻¹ (peak uprising). CytC: 5 mg mL⁻¹, 0.5 M Tris-HCl buffer (pH 7.4).

additive), and the two lower curves that merge with the first one for SAMs with $n=6$ and 11, represent kinetic data obtained in the presence of glucose at 200 and 400 g L⁻¹ (at a higher solution viscosity, *vide infra*), respectively (for corresponding numerical values see Table 1). Figure 2 demonstrates an evident independence of the rate constant for SAMs with $n=2$ and 3. This plateaulike region, although it spans only two CH₂ units, is well pronounced (Miller et al.

Table 1. Values of diffusion coefficients and heterogeneous standard rate constants for CytC electron exchange at Au electrodes modified by hydroxy-terminated *n*-alkanethiol SAMs ($n=2, 3, 4, 6, 11$) under variable solution viscosity. The values are averaged over 3 to 5 independent experiments with a maximum error within 5%.

Glucose [g L ⁻¹] (M)	Relative viscosity (η_r)	$D_0 \times 10^7$ [cm ² s ⁻¹]	k^0 [cm s ⁻¹]					
			$n=2$ (Tris)	$n=3$ (Tris)	$n=4$ (Tris)	$n=6$ (Tris)	$n=11$ (Tris)	$n=3$ (Phosph)
0 (0)	1	8.02	2.065×10^{-2}	2.00×10^{-2}	6.0×10^{-3}	8.6×10^{-4}	5.76×10^{-6}	2.77×10^{-2}
100 (0.56)	1.33	5.98	–	1.45×10^{-2}	4.8×10^{-3}	–	–	1.90×10^{-2}
200 (1.12)	1.80	4.91	1.075×10^{-2}	1.00×10^{-2}	3.7×10^{-3}	8.4×10^{-4}	–	1.44×10^{-2}
300 (1.67)	2.63	2.95	–	6.99×10^{-3}	2.8×10^{-3}	–	–	1.10×10^{-2}
400 (2.24)	3.96	1.84	4.708×10^{-3}	4.77×10^{-3}	2.0×10^{-3}	8.6×10^{-4}	5.82×10^{-6}	6.79×10^{-3}

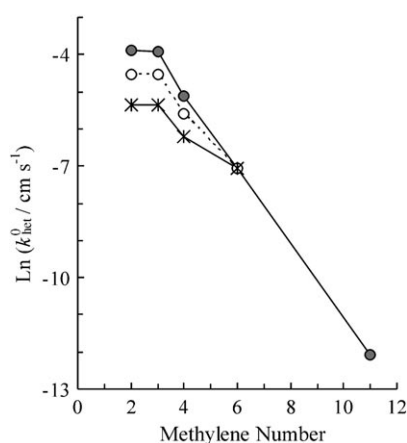


Figure 2. Logarithm of the heterogeneous standard rate constant for CytC electron exchange at Au electrodes modified by hydroxy-terminated *n*-alkanethiol SAMs ($n=2,3,4,6,11$) versus methylene unit number under variable solution viscosity. Upper curve (filled circles): no viscous additive, $\eta_r=1$; middle curve (open circles), $\eta_r=1.80$; lower curve (asterisks) $\eta_r=3.96$ (note all three curves merge at $n=6$ and 11, and form a single sloped line).

indicated essentially the same result in their pioneering yet incomplete report^[25]. Actually, it is much smaller compared to analogous plateau regions in cases in which CytC exhibits an irreversibly adsorbed kinetic pattern, with ω -COOH (span over nine CH₂ units^[26,29]) and ω -Py (span over 14 CH₂ units^[27,29]). At the same time, our results corresponding to larger electrode-reactant separations (SAMs with $n=6$ and 11), demonstrate an exponential decay of the rate constant [Eq. (5)] with a slope of about 1 per CH₂ unit. This is in excellent agreement with previous results obtained for various bioelectrochemical and matching model systems (involving either irreversibly adsorbed or freely diffusing redox species). The points for $n=4$ apparently fall in the intermediate region. This becomes clearer on considering this issue and the high-pressure and viscosity effects altogether (vide infra).

It is natural to interpret the change in the dependency mode of $\ln(k_{\text{het}}^0)$ on n , Figure 2 (or on the CT distance estimated in Å, see below), in terms of a “mechanistic change-over” as it has been suggested in the case of bound CytC;^[29,32b] however, other interpretations have also been suggested.^[26,30] There is a common opinion on the origin of the exponentially sloped region (wherever it appears on the variation of n) that it is due to the nonadiabatic regime of

CT^[23a–30,33,42] (also known as a long-range tunneling or super-exchange mechanism^[41,42]). Furthermore, two different patterns for the plateau region have mainly been discussed so far (based solely on the data for the bound CytC available at that time^[24,28,30a,b]). In particular, on the basis of the unified theoretical CT model,^[37–40] some of us interpreted the onset of the plateau region in terms of a changeover to the adiabatic (friction controlled) intrinsic mechanism (without invoking any change in the CT rate-determining step as such).^[30,32] The adiabatic mechanism implies control of CT by the protein’s conformational dynamics through direct intrinsic coupling between these events occurring in one inseparable (bio)chemical act (vide supra). In contrast, another frequently discussed interpretation considers the conformational rearrangement (that can be viscosity-sensitive) to be intrinsically separated from the CT event, taking place in the preceding stage, that is, an essentially different elementary barrier-crossing stage.^[24a,27a] Serious arguments that dispute the latter version (at least, concerning the CT mechanism for CytC in bioelectrochemical systems) are presented elsewhere.^[30,32] The data of Figure 2 and Table 1 (together with the data on the HP effects presented below) seemingly give extra support to the interpretation that implies a changeover in the intrinsic CT mechanism rather than the model that implies an essential change in rate-determining step (see references [54,55] for the mechanistic classifications). Indeed, it would be difficult to assume an existence of a rate-determining (and viscosity-controlled, vide infra) large-scale rearrangement of the protein–SAM moiety (gating mechanism) for the case of freely diffusing CytC, in the absence of tight interactions between these items^[56] (see also the next sub-section). The comparison with the matching kinetic results obtained for CytC irreversibly bound to SAMs would offer some new insights. It is difficult to compare directly heterogeneous (reference [25] and present case) and unimolecular^[24,26–30] standard rate constants, k_{het}^0 and k_{ET}^0 [Eq. (1)] with the dimensions of cm s⁻¹ and s⁻¹, respectively, since the actual value of the pre-equilibrium constant (K_A) in Equation (1) is unknown.^[25] However, the previous scarce data for SAMs encountering free CytC suggest that the interaction is slightly attractive^[25] and would lead to some enrichment of a diffuse part of the double layer in the vicinity of the ω -OH groups with CytC compared to the bulk solution (note, it is assumed throughout that the effective concentration of CytC is almost constant throughout the SAM series with n running from 2 to 11). Certainly, the

weak attractive interaction should be distinguished from the irreversible adsorption, as is manifested through essentially different CV responses (see Experimental Section and, for example, references [23–27,29,33]). However, a sound comparative analysis of the “effective” protein-to-terminal group distances for freely diffusing and adsorbed CytC is possible by the direct resembling of “apparent turnover points”, that is, the formal CT distances at which the mechanistic changeover occurs. The previous comparison of such turnover points for CytC operating at ω -Py and ω -COOH SAMs, indicated that the “effective” CT distance (more precisely, its part due to the protein/terminal group junction) for the case of ω -COOH SAMs is about 5 Å larger as compared to ω -Py SAMs.^[29b] For the latter system the protein/SAM junction thickness can be considered to provide a zero contribution to the overall “effective” CT distance due to the “direct wiring” of ω -Py to the heme iron.^[27b] Now, comparing the “turnover points” for the ω -Py (a reference system)^[28,30] and ω -OH (present study, Figure 2) cases, one can estimate the additional “effective” CT distance of about 10–11 Å compared to the “directly wired” case, and about 5 Å as extra distance compared to the electrostatically adsorbed case of ω -COOH SAMs. These estimates, when considered together with the results of previous calculations,^[29b,33a] yield the values for a variable electronic coupling, H_{if} , ranging from approximately 3 cm⁻¹ for the case of $n=2$ ($R_{\text{eff}} \approx 15$ Å) to about 0.02 cm⁻¹ for the case of $n=11$ ($R_{\text{eff}} \approx 25$ Å), assuming $H_{if}^{(0)} \approx 1600$ cm⁻¹ at the hypothetical closest separation distance, $R_0 \approx 2.6$ Å.^[20,29,33a] The estimated CytC- ω -OH “effective” separation distance of 10–11 Å seems very reasonable if one assumes that the freely diffusing regime is made possible through the loosely bound CytC forming the solvent-separated encounter complex with ω -OH, as it was found in the case of thermal- and photoinduced CT within the “charge-modified” complex of photosynthetic reaction center (PRC) and cytochrome c_2 ,^[5] and from the artificial Ru-coordinated polypeptide electron donor to ferri-CytC^[4b] (see also further discussion below).

Impact of stabilizing/denaturing additives on the kinetic and thermodynamic patterns of free CytC: Figure 3 shows typical CV curves as the electrochemical response for a freely diffusing CytC at ω -OH SAMs in the presence of glucose (0, 0.56, 1.12, 1.67, and 2.24 M; Figure 3a), urea (0, 4, 6, and 8 M; Figure 3b), and pyridine (0.6 M; Figure 3c). The extracted kinetic parameters, including standard rate constants

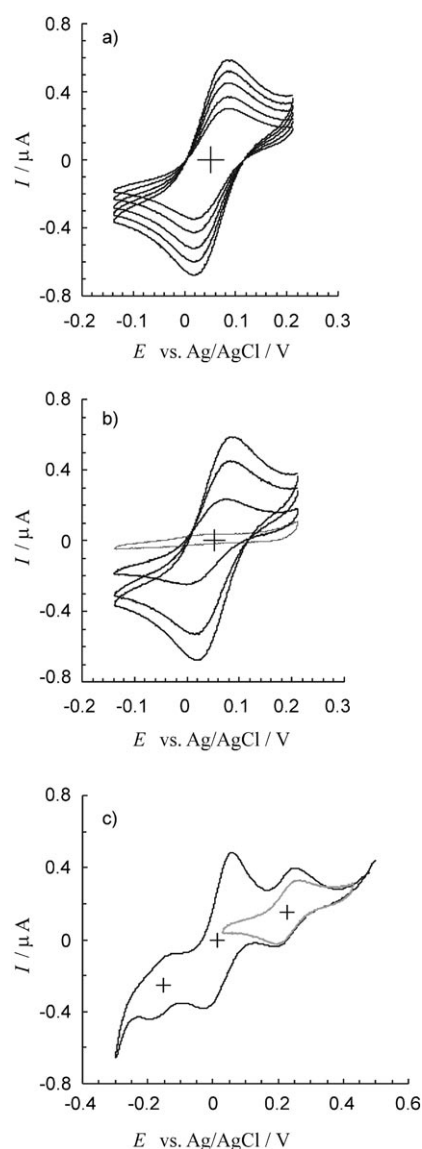


Figure 3. CVs for CytC electron exchange at Au electrodes modified by hydroxy-terminated n -alkanethiol SAMs with $n=3$: a) at different concentrations of glucose, 0, 200, 300, and 400 g L⁻¹, respectively (peak decline); b) at different concentrations of urea, 0, 4, 6, and 8 M, respectively (peak decline); c) at 0.6 M pyridine (triply split curve) and 8 M urea (simple curve, right-hand side); ambient pressure, scan rate: 0.05 V s⁻¹.

(k_{het}^0) and diffusion coefficients (D_0), of CytC are presented in Table 2. The dependencies of $\ln(k_{\text{het}}^0)$ on the molar con-

Table 2. Values of relative viscosity, diffusion coefficients, and heterogeneous standard rate constants for CytC electron exchange at Au electrodes modified by hydroxy-terminated n -alkanethiol SAMs ($n=2, 6$) under the variable urea concentration. The values from literature data and the corresponding variants are given in italics (see the footnotes and text for details).

Urea [M]	Relative viscosity ^[a] (η_r)	Formal potential (E^0) [mV]	$D_0^{\text{eff}} \times 10^7$ ($D_0^{\text{corr}} \times 10^7$) [cm ² s ⁻¹]	$k_{\text{het}}^0 \times 10^2$ [cm s ⁻¹] ($n=3$)	$k_{\text{het}}^0 \times 10^4$ [cm s ⁻¹] ($n=6$)	$D_0 \times 10^7$ ^[c] [cm ² s ⁻¹]	$k_{\text{het}}^0 \times 10^2$ ^[d] [cm s ⁻¹] ($n=3$)	$k_{\text{het}}^0 \times 10^4$ ^[d] [cm s ⁻¹] ($n=6$)
0	1	52	8.0	2.50	9.25	12.0	3.06	11.3
2	1.01	50	7.9 (7.8) ^[b]	1.83	6.76	8.8	2.02	7.47
4	1.22	48.5	5.8 (7.0) ^[b]	1.31	3.73	6.4	1.38	3.92
6	1.41	35.5	1.1 (6.2) ^[b]	0.44	0.88	3.0	0.74	1.48

[a] Data from references [23b,64]. [b] Calculated by using the mean relative amounts of the His/Met-ligated CytC.^[23b,63] [c] Simulated data from reference [23b] (entries corresponding to 2 and 4 M urea are interpolated values). [d] Calculated by using diffusion coefficients of reference [23b].

centrations of the glucose and urea additives are plotted in Figure 4. The experimental data with pyridine (Py) as an additive only have illustrative character because of restrictions in accurate determination of kinetic parameters (caused by a strong overlap of individual CV waves representative of three coexisting CytC conformers, Figure 3c, *vide infra*). Both Figure 4 and Table 2 show that in urea-implicated solutions the standard rate constant declines unsteadily in a sim-

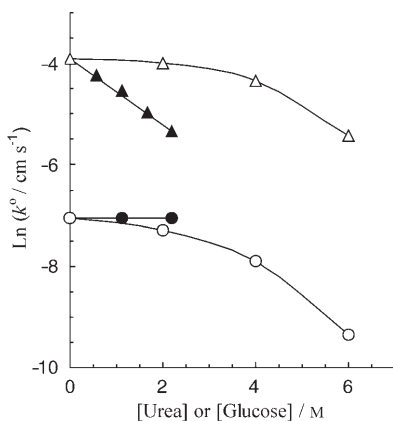


Figure 4. Semilogarithmic plots of the heterogeneous standard rate constant for the CytC electron exchange at Au electrodes modified by hydroxy-terminated *n*-alkanethiol SAMs, *n*=3 (triangles) and 6 (circles), versus the concentration of additives, glucose (closed symbols) and urea (open symbols).

ilar manner for the cases of ω -OH SAMs with *n*=3 and 6. Interestingly and importantly, the same figure shows that the decline in the rate constant is more steep and essentially monotonic in the case of glucose additives at *n*=3, as well as at *n*=2 (not shown here, see Table 2), but is totally absent with glucose at *n*=6, as well as at *n*=11 (not shown here, see Table 2). The data analysis shows that changes in the FSCV response of “free” CytC in the presence of glucose additives (Figure 3a) are manifested mostly through the decline in peak current, indicating a systematic decline in the diffusion coefficient due to the increase in solution viscosity. It is unlikely that any increase in the effective radius of the CytC globule contributes to the observed effect on D_0 , because viscous additives are known to stabilize proteins’ native-like conformation (*vide infra*) and even reduce their effective radii.^[57] This kind of squeezing is somewhat analogous to the pressure-induced squeezing and stabilization at moderately HP (up to 150–200 MPa) of proteins and probably is due to the collapse of a free volume within the protein globules (*vide infra*).^[58]

The global (but not local, see below) thermodynamic stability issue of CytC can directly be accessed through the DSC studies. In the present work, the DSC experiments were performed in parallel with the bioelectrochemical kinetic ones. The micro-calorimetric (protein thermal melting) curves for “free” CytC in the presence of the same concentrations of glucose (with minor variations) and urea are de-

picted in Figure 5, and the corresponding thermodynamic parameters are collected in Table 3. Our calorimetric data indeed show the stabilization effect at all glucose concentrations applied (Figure 5a). In general, we observed splitting

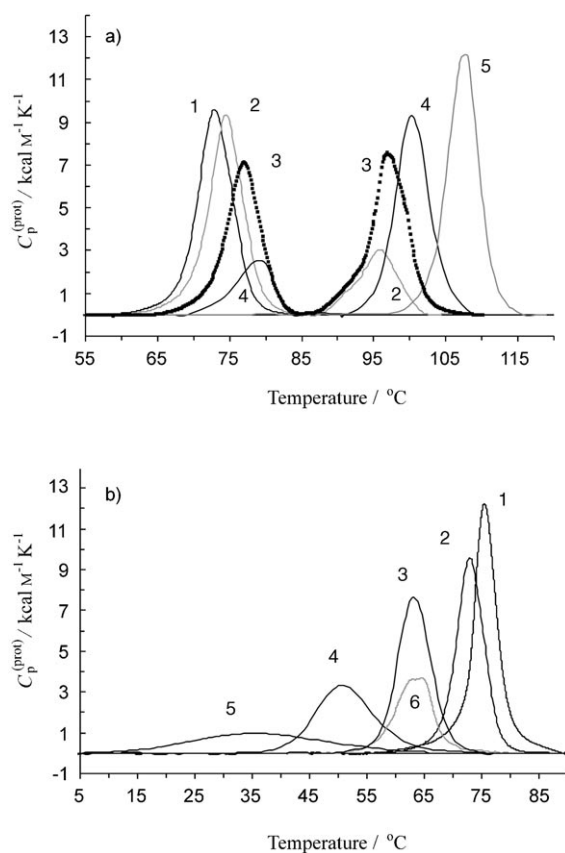


Figure 5. DSC melting curves: a) CytC in Tris-HCl buffer, in the presence of glucose, 0 (1), 100 (2), 200 (3), 300 (4), and 600 g L^{-1} (5); and b) in 2 mM phosphate buffer with 0.5 M KCl added (1) and in Tris-HCl buffer, in the presence of 0 (2), 2 (3), 4 (4), and 6 M (5) urea, and 0.6 M pyridine (6).

of melting endothermic peaks in two components, indicative of two different mechanisms of protein stabilization by glucose (as also discussed in the literature^[59]). We define the two mechanisms of stabilization as mechanisms I and II as to refer to low- and high-temperature peaks observed. The melting curves depicted in Figure 5a were recorded after the overnight equilibration of solutions exploited. An increase in the equilibration time shifts the slowly drifting quasi-equilibrium between forms I and II in favor of the latter form, such that after three days of equilibration almost only form II could be observed (not shown here). Hence, all the kinetic experiments with the glucose additives were performed after the lengthy periods of equilibration to ensure the single, more efficient, stabilization regime (mechanism II). While using the glucose additives, the different response of the rate constant regarding the SAM thickness evidently is not caused by the thermodynamic effect of stabilization, because at *n*=6 and 11 the CT rate constant is in-

Table 3. Thermodynamic parameters (see text) for CytC thermal melting in the presence of different additive type and concentration. 500 mM Tris-HCl buffer was used throughout unless otherwise indicated.

Solution	Peaks	T_m [°C]	ΔT [°C]	$C_{p(m)}^{(prot)}$ [kcal mol ⁻¹ K ⁻¹]	ΔH_{cal} [kcal mol ⁻¹]
phosphate (20 mM + 0.5 M KCl)	single	75.5	4.4	12.3	70.8
Tris HCl 500 mM (no additives)	single	72.9	5.5	9.6	60.5
+ urea 2 M	single	63.1	6.9	6.5	54.5
+ urea 4 M	single	50.9	11.5	3.3	43.6
+ urea 6 M	single	36.2	27.0	0.72	25.6
+ glucose 0.56 M	1	74.6	5.3	9.0	56.0
	2	95.8	6.3	2.9	19.3
+ glucose 1.12 M	1	76.9	5.2	7.1	43.4
	2	96.7	5.5	7.5	47.5
+ glucose 1.68 M	1	78.7	6.3	2.5	15.9
	2	100.3	5.1	9.2	55.7
+ glucose 3.36 M	single	108.0	4.6	12.1	69.9
+ pyridine 0.6 M	split	ca. 64–65	7.1	3.7	30.8

sensitive to the glucose concentration, see Figure 4 (at otherwise similar conditions except the different electronic coupling). Rather the observed decline at $n=2$ and 3 (and partially for $n=4$, vide infra) seems to be due to the dynamic viscosity effect caused by the frictional mechanism discussed above [Eq. (6)] that transforms into the viscosity-insensitive nonadiabatic mechanism for thicker SAMs [Eq. (5), vide infra].

In contrast with the case of glucose, Figure 5b indicates significant destabilization of “free” CytC with an increase in urea content, and in this case full thermodynamic equilibration of the system takes place within a few minutes. The protein melting (endothermic) peak as a whole gradually shifts to lower temperatures and broadens significantly, becoming totally undetectable at the urea concentration of 8 M (not shown in Figure 5b). This kind of calorimetric behavior is characteristic for the “molten-globule” (MG) or “molten-globule-like” states in which the protein’s tertiary structure is still rather compact and native-like, but significantly labilized, undergoing large-scale fluctuational motions.^[12–15] The MG-like states of globular proteins induced by urea and its derivatives at different pH are well-known.^[14] Actually, the MG state or series of MG-like states can be formed by the moderate action of any denaturing factor (including temperature) or their combinations.^[7b, 12–14]

Certain earlier work was devoted to bioelectrochemical studies of CytC under the destabilizing conditions caused by low-molecular-weight additives, such as urea, pyridine, and so forth.^[23b, 60–62] In this work,^[23b] the influence of denaturants, particularly urea, was interpreted in terms of the effect that results in a variable, [urea]-dependent equilibrium between the native-like Met80-Fe^{III} and non-native (mostly bis-His-Fe) folded states, in which the native-like Fe^{III} coordination is actually deemed as equivalent to the global native fold of CytC as such. However, as it was demonstrated by Antalík et al.,^[8] the local stability of a Met80-Fe^{III} bond does not necessarily follow the trend of global thermodynamic stability of this protein. From our results depicted in Figure 5b, it follows that above the urea concentration of about 4 M, the CytC conformation is already notably altered,

not to say anything about the situation for the 6 M urea solution, for which the cooperative character of the calorimetric melting peak is almost lost. The above-mentioned investigations^[23b, 60–62] as well as other results^[63] report 67 to 96% “native” folding of CytC (implying the global conformation) under these conditions (6 M urea), which seems highly questionable in the light of our calorimetric results, which directly indicate that the global conformation is strongly altered throughout. The most

reasonable interpretation of the earlier^[23b] and present (this work) experimental findings should imply that in a global MG-like state of CytC, the successive increase in fluctuational mobility (with increasing urea concentration) of the tertiary structure (that remains on average still compact) allows for a “chemical-like” equilibrium between the native-like and nonnative local folding of the metal coordination that is observed by optical, NMR, and fluorescence spectroscopy, and so forth.^[23b, 63] Indeed, only the decline in D_0 of approximately 1.4 times (in 6 M urea solution) can be attributed to the increase in viscosity.^[64] An additional decline in D_0 of about 1.15–1.3 times (for the same solution) can be attributed to the increase of the Stokes radius due to the transformation to the global MG-like state.^[15b] The rest of approximate four- to fivefold decrease could be attributed to the decrease in the effective concentration of native-like His/Met heme-ligation fold in the (global) heavily altered MG-like state in which the local native-like fold still persists at 20 to 25% under these particular experimental conditions (500 mM Tris-HCl, 6 M urea). This estimate is in reasonable agreement with earlier estimates^[23b, 60–62] if one implies the local heme-related rather than the global native fold, and takes into account the data dispersion due to different solution compositions and methodologies applied.

However, this interpretation disregards the small changes (ca. 17 mV drop) in the “initial” CytC redox potential attributable to the “native” local fold (+520 mV). As an alternative interpretation, the observed small potential drift may reflect the weakening of an interaction between the iron-bound Met80 and Tyr67, possibly indicative of an increased distance between the 60 s helix and the heme group (Tyr67 is known to affect the heme redox potential of CytC, since it modulates the Met80-heme-iron bond strength).^[8b] Both possibilities were considered in calculations of k_{het}^o for the urea-implicated pattern and it was found that both models result in a substantial decrease in the rate constant (Table 1).

The decline in k_{het}^o with increasing urea concentration in both cases of thin ($n=3$) and thick ($n=6$) SAMs (otherwise exhibiting diverse behavior regarding the variable pressure

and the glucose content, *vide infra*), indicates that this effect is not due to the intrinsic mechanism, but rather to the pre-equilibrium constant, K_A [Eq. (1); however, K_A should again remain constant over the series with other variables, *vide infra*]. This peculiarity can be interpreted in terms of an increasingly unfavorable interaction of free CytC with the SAM ω -OH groups in the sequence of molten-globule-like states. This could be due to the increase in “delocalization” of the protein’s effective surface charge (associated with the large-scale conformational fluctuations) with increasing urea concentration. Figure 6 demonstrates the impact of different

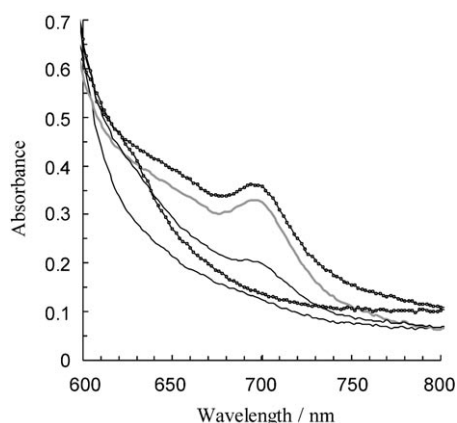


Figure 6. An impact of different additives on the 695 nm CT band due to the Met80/Fe^{III} native fold. From top to bottom: no additives; 400 g L⁻¹ glucose; 6 M urea; 8 M urea, and 0.6 M pyridine.

additives on the 695 nm CT band attributable to the S(Met80)–Fe^{III} axial bonding, being an indicator of local Met80–Fe native ligation in CytC.^[23,60–62] One can see that in a 2.24 M glucose solution, the native-like local fold is not altered. In a 6 M urea solution, the band is still observable, in agreement with either of two models for local rearrangements discussed above. At the 8 M urea concentration level, the CV response at the “native” formal potential almost disappears (Figure 3b), and resembles an apparent disappearance of the melting peak in the calorimetric response (Figure 5b) and a disappearance of the 695 nm CT band (Figure 6), indicating total loss of the local native fold. Instead, the CV response with the midpoint potential at 211.5 mV appears to be indicative of the substitution of Met80 by some nonnative ligand (the candidates are one of the “surface” Lys groups, water, etc.; Figure 3c; see also, for example, references [23, 60–62]).

We also briefly consider the impact of 0.6 M pyridine on the kinetic and thermodynamic patterns of free CytC (a typical concentration used in the earlier work^[61b]). From the CV response (Figure 3c) one can deduce the presence of three different forms. Inspection of Figure 5b shows that neither of them is native-like, because the protein melting endotherm is, although slightly split, entirely shifted and indicates significant destabilization (comparable with the urea-induced MG-like forms, Figure 5b). No sign of the

native-like conformation remains on the thermogram. It follows from Figure 6 that in all those forms Met80 is substituted by nonnative ligands.^[23,60–61] The realistic candidates are Py itself, one of the “surface” Lys groups, and a water molecule. The total coincidence of midpoint potentials for component III detected in the presence of 0.6 M Py and at 8 M urea concentration, respectively (Figure 3c), could be an indication of a similar local (but in no case of the global) protein folding in these two cases.

Impact of hydrostatic pressure on the kinetic pattern of free

CytC: Semilogarithmic dependencies of k_{het}^0 on the hydrostatic pressure up to 150 MPa for SAMs with $n=3, 4,$ and $6,$ are depicted in Figure 7a–c, respectively. It can be seen that in the case of SAM with $n=3,$ the value of $\ln(k_{\text{het}}^0)$ decreases

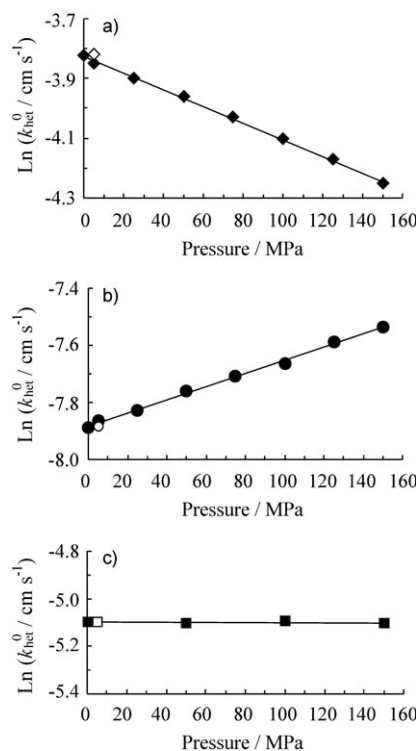


Figure 7. Logarithm of the heterogeneous standard rate constant for CytC electron exchange at Au electrodes modified by hydroxy-terminated *n*-alkanethiol SAMs ($n=3, 4, 6$) versus hydrostatic pressure, a) $n=3$; b) $n=6$; c) $n=4$.

linearly with pressure, yielding, according to Equations (6) and (9), a positive volume of activation of $+6.7 \pm 0.5 \text{ cm}^3 \text{ mol}^{-1}$ (see also Tables 4 and 5). This value is essentially similar to $+6.1 \pm 0.5 \text{ cm}^3 \text{ mol}^{-1}$ found in the case of 4,4'-bipyridyl- and 4,4'-bipyridyldisulfide-modified Au electrodes (also considered as thin SAMs).^[30c] In contrast, for a much thicker SAM with $n=6,$ we found that the value of $\ln(k_{\text{het}}^0)$ increases linearly with increasing pressure to yield a negative volume of activation of $-5.5 \pm 0.5 \text{ cm}^3 \text{ mol}^{-1}$, Figure 7b. Hence, for the first time, the change in sign for the activation volume has been detected for an essentially simi-

Table 4. Values of heterogeneous standard rate constants for CytC electron exchange at Au electrodes modified by hydroxy-terminated *n*-alkanethiol SAMs (*n*=3, 4, 6) under variable pressure. The standard error within the given pressure cycle was less than ±3% (see the “return” entries), the absolute error in the rate constant determination (independent series): ±10%.

SAM pressure [MPa]	0	5	25	50	75	100	125	150	5 (return)
$n=3$ $k_{\text{het}}^o \times 10^2$ [cm s ⁻¹]	2.19	2.13	2.02	1.91	1.78	1.66	1.55	1.43	2.21
$n=6$ $k_{\text{het}}^o \times 10^4$ [cm s ⁻¹]	3.74	3.85	3.98	4.27	4.48	4.69	5.05	5.33	3.77
$n=4$ $k_{\text{het}}^o \times 10^3$ [cm s ⁻¹]	6.12	6.14	–	6.07	–	6.13	–	6.075	5.73

Table 5. Experimental volumes of activation [± 0.5 , in cm³mol⁻¹] for CytC electron exchange at Au electrodes modified by hydroxy-terminated *n*-alkanethiol SAMs (*n*=3, 4, 6) under variable hydrostatic pressure, and estimated values of different contributing terms (in the same units).

SAM	$\Delta V_{\text{a(exp)}}$	$1/4(\partial\lambda/\partial P)_T$	$RT(\partial\ln\eta/\partial P)_T$	$\beta RT(\partial R_{\text{e}}/\partial P)_T$
$n=3$	+6.7	–(2 to 3)	+(8 to 10)	(0)
$n=6$	–5.5	–(2 to 3)	(0)	–(2 to 3)
$n=4$	–0	–(2 to 3)	+(4 to 5)	–(1 to 2)

lar biochemical system as a result of the predominant variation of a single parameter, namely, electronic coupling. In the case of a SAM with *n*=4, an intermediate behavior is displayed with no effect of pressure on k_{het}^o , yielding $\Delta V_{\text{a}} \approx 0$, Figure 7c and Tables 4 and 5.

In previous work^[32a] it was mentioned for the first time that due to the exceptional property of water not to change its viscosity with pressure around room temperature, HP kinetic studies of biochemical processes provide a unique possibility to vary the protein's intrinsic viscosity without altering the viscosity of the external (bulk) water (although the solvating or “bound” water should be considered as part of the protein molecule^[17,18]). The above-mentioned property of water is probably due to the peculiar multicomponent nature of this liquid.^[65] Thus, moderately high pressure (up to 200–300 MPa) affects those structural components that are not responsible for transport properties including fluidity and diffusion.^[66] At the same time, according to numerous experimental and theoretical studies, the protein's interior, especially peripheral regions forming the unified fluctuating dynamic system together with and “slaved” by the interfacial (cooperative water–glucose, vide infra) assembly, can be viewed as a highly heterogeneous viscous liquid rather than a dissolved, solidlike macromolecular substance.^[16–18,67,68] The effective viscosity of such a complex “liquid”, like any other liquid mixtures, should increase with pressure due to a universal mechanism of increasing intrinsic friction. Although, it has been well-established that proteins tend to denature under high-pressure conditions above 200–300 MPa,^[69] proteins normally attain native-like conformation for moderately variable pressure (below 150–200 MPa).^[70] In particular, CytC was shown to be increasingly stabilized by high pressure under 220 MPa provided that the ordinary pH conditions were held.^[58b] This fact is in remarkable agreement with the above proposal regarding the increase in internal protein friction under pressure (within the pressure limits applied in the present work; see also ref-

erence [58] and further discussion below). Importantly, according to the available data, the increased hydrostatic pressure and stabilizing additive (glycerol) both lead to a decrease in the protein “free” volume.^[57,58] In this context, our HP kinetic experimental data nicely agree with the theoretical predictions for both adiabatic and nonadiabatic bioelectrochemical CT made above. Indeed, Equation (9) predicts a substantially positive activation volume due to the increase in viscosity (friction) in the vicinity of the redox center. In the case of a protein globule as reaction medium that mainly has properties of a viscous liquid or a mixture of such liquids,^[67,68] a large positive contribution due to the first term in Equation (9) can be expected.^[32a,49a]

The second term due to variation of the outer-sphere reorganization energy (Franck–Condon) factor, when considered as originating from the effect of pressure on the bulk dielectric properties of external water, can be predicted to amount to about –4 to –6 cm³mol⁻¹, assuming that λ amounts to approximately 1 eV (–20 to 25 kcal mol⁻¹) and originates completely from the bulk properties of water.^[50–53] In the case of CytC reactions at SAMs [for which, in general, Eq. (10) is approximately valid], the overall value of $\lambda = 0.6–0.8$ eV is roughly composed of a roughly 50% “outer-sphere” (solution) component that can contribute about half of the activation volume, and another roughly 50% of the “inner-sphere” protein reorganization component (Franck–Condon term) found to be negligibly altered by pressure, and therefore does not contribute to the activation volume.^[51a] Note that the same can be concluded for the contribution from the SAM interior ($\lambda_{\text{SAM}} \sim 0$), since it can be assumed that $\epsilon_{\text{s}} = \epsilon_{\infty}$.^[53] Thus, the most probable overall contribution of the second term of Equation (9) would be –2 to –3 cm³mol⁻¹. This value, together with the overall experimental value of +6.7 cm³mol⁻¹ yields the value of the frictional term, namely, +8 to +10 cm³mol⁻¹ (Table 5). We stress again that this contribution originates from the direct influence of hydrostatic pressure on the intrinsic protein friction (viscosity).

On considering the nonadiabatic mechanism, Equation (8), it is seen that the second term due to the Franck–Condon factor may again contribute about –2 to –3 cm³mol⁻¹. This value together with the overall experimental value of –5.5 cm³mol⁻¹ yields for the first term (related to the effect of squeezing the system) a value of about –2 to –3 cm³mol⁻¹ (Table 5). This kind of contribution to the overall volume of activation has actually been predicted for protein systems.^[51b] Note that the overall pressure pattern implies dynamic squeezing of the protein, manifested either through the increase in internal friction or shortening of the CT distance, depending on the intrinsic CT regime. Formally, one can argue that some squeezing of the system takes place already in the pre-equilibrium stage, Equa-

tion (1). Although the corresponding equilibrium constant (K_A) contains some terms known to weakly depend on pressure, the contributions of which tend to cancel each other out,^[49] even the hypothetical possibility of this event does not change the main conclusion concerning the mechanistic changeover. However, in a general sense, the possible hindering role of the pre-equilibrium term will be discussed in the last section. On going to the pressure effect for a system with $n=4$, tentatively assigned to fall into the intermediate regime, it was found that the experimental activation volume is virtually zero ($\Delta V_a \sim 0$). This value is almost half-way between the values found for $n=3$ and $n=6$, namely, $0.6 \pm 1 \text{ cm}^3 \text{ mol}^{-1}$. Table 5 summarizes the ranges of estimated values for the individual contributing factors to the experimental ΔV_a for the cases of both observed mechanisms and in the intermediate regime, which are in a good mutual agreement. Consequently, we conclude that our activation volumes obtained from HP kinetic experiments are in good agreement with the results obtained through other approaches, and therefore have a predictive power of high confidence.

Links between the solution (external) versus the intraglobular viscosity, the protein's thermodynamic stability, and dynamic slaving: Returning now to the effect of external viscosity (Figure 8, Table 1), one can mention that for SAMs with $n=2$ and 3, formally “full” frictional control is realized [$\delta \approx 1$, Eq. (6)], normally characteristic for redox species in which the redox-active (typically metal complexes) center is immediately solvated by the aqueous medium.^[33a,40–43] In the case of biochemical processes occurring inside the protein environment, the viscosity control takes place through Equation (6) in which usually $0 < \delta < 1$.^[22,27a,30b,44–46] The “maximum” value of about 0.6 was detected in the case of specific adsorption on the Py-terminated thinner SAMs (plateau region).^[29b] Somewhat larger slopes were found in the case of a CT within the “homogeneous” (solution) system

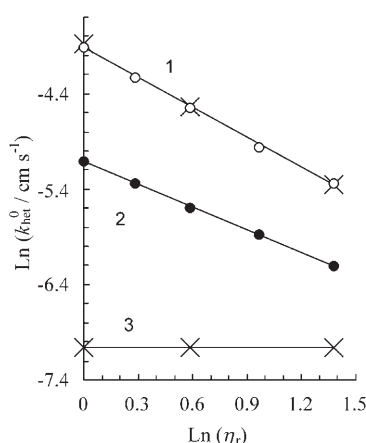


Figure 8. Logarithm of the heterogeneous standard rate constant for CytC electron exchange at Au electrodes modified by hydroxy-terminated n -alkanethiol SAMs versus logarithm of the solution viscosity. Plot 1: two coinciding plots for $n=2$ (crosses) and $n=3$ (open circles); plot 2: $n=4$ (closed circles); plot 3: $n=6$ (crosses).

involving zinc-substituted CytC, and wild-type and mutant cupriplastocyanin, ranging from 0.7 to 0.9.^[21] Interestingly, full viscosity control ($\delta \approx 1$) has been observed for photo-induced CT from the artificial Ru-coordinated polypeptide electron donor to ferri-CytC,^[4b] occurring through the loosely bound (encounter) complex, as opposed to the “preformed” (tight) complex involving the same reactants ($\delta \approx 0.6$), both patterns being observed to occur simultaneously. The latter findings closely match the whole pattern regarding CytC bioelectrochemical CT in both the tightly bound and freely diffusing (to Au-deposited SAMs comprising ω -COOH and ω -OH) regimes, respectively. In addition, recent experimental and computational results obtained for a related system, the “charge-modified” complex of the photosynthetic reaction center (PRC) and cytochrome c_2 ,^[5] strongly suggest formation of a solvent-separated, softly stabilized complex as an encounter reactive associate (vide supra).

To explain the observed deviation of δ from unity (provided the intermediate regime is excluded, see reference [30b] and the present work), earlier research suggested that the overall “effective” friction that controls the process, additively originates from both solvent and protein components, and operates through Equation (11),^[68] in which C is a constant, and σ represents the protein's intrinsic viscosity.

$$k_{AD} = \frac{C}{\sigma + \eta} \exp\left(-\frac{\Delta G_a}{RT}\right) \quad (11)$$

However, from this approach it follows that for cases in which, for example, $\delta \approx 0.5$ – 0.8 , the external (solution) and protein interior contribute comparably (the ratio σ/η amounts only to ca. 2 to 4), which is highly questionable because the protein interior is known to be much more viscous compared to bulk water, or even compared to aqueous solutions containing conventional viscous additives.^[29b,44–46,67] At the same time, in the cases where $\delta \approx 1$ (as in the present case), this model suggests that $\sigma \approx 0$, which implies that there is no frictional effect from the protein interior at all. Evidently, such a conclusion contradicts the existing viewpoint about the protein's internal dynamic properties and does not agree with our HP and other complementary kinetic results that convincingly revealed an essential role of the protein's intrinsic friction (for further criticism of Eq. (11), see reference [16a]). In this context, the earlier work that allowed the reliable estimation of an intrinsic effective relaxation time of CytC controlling adiabatic CT, namely about 200 ps, should be mentioned.^[29b,55b] This rather slow relaxation time roughly corresponds to an approximate 1000-fold enhanced intrinsic “effective” friction compared to the bulk aqueous environment.

The question emerges on how the moderate variation of external viscosity can alter the highly exceeding internal viscosity so effectively? The answer can be found in a recently introduced concept of dynamic “slaving”^[17] that implies that “solvent fluctuations dominate protein dynamics and function”.^[16b] Indeed, for another well-studied “model” protein,

myoglobin, it has been established that several of its dynamic features (including the rate constants of functional elementary processes, $k_F(T)$) change parallel with the rate coefficient of the solution's dielectric fluctuations, $k_D(T)$, such that,^[16] $k_D(T)/k_F(T) \approx m = \text{constant}$, in which, for different events, m varies within the range of 3×10^2 to 3×10^4 (with a logarithmically averaged value of ca. 10^3). The origin of such a subordination of intrinsic conformational relaxation time to the external macroscopic counterpart characteristic (bulk dielectric relaxation), should lie in a cooperative effect of simultaneous multisite interaction of the solvent components (water, sugar, glycerol, etc.) with charged and polar groups on the protein surface.^[16,59,67c,68b] Indeed, numerous studies indicated the essential role of protein solvation in the triggering and further tuning of their dynamic characteristics and functions.^[16–18,67–68] However, the close protein–sugar interaction does not imply primitive replacement of a bound water from the protein's first solvation sphere. Our calorimetric results suggest that the protein–glucose (in general, protein–sugar or protein–polyol) interactions, in contrast to the respective protein–urea counterpart, are of essentially cooperative character and may indeed result in the slow and specific penetration of glucose within the close vicinity of the protein–solution interface, as demonstrated for a lysozyme/water/trehalose system in recent molecular dynamics studies.^[71] Our finding that CytC under the present conditions (weak interaction with SAM terminal groups) exhibits a totally dependent behavior ($\delta = 1$), compared to the case in which it is (specifically) tightly adsorbed at the surface ($\delta \approx 0.6$ ^[29b]), confirms such a conclusion. Furthermore, it suggests that when the external solution is screened due to the tight protein/SAM contact (that mimics the protein–membrane or protein–protein multisite contact), the slaving effect is not complete due to the lack of the full protein–solution interaction.

Finally, our calorimetric data revealed thermodynamic stabilizing effects of glucose upon the native conformation of CytC that correlates with the dynamic frictional (viscosity) control in the adiabatic kinetic regime [manifested through Eq. (6)]. This observation is in a remarkable agreement with the recent result of Chalikian et al. for the stabilizing effect of pressure on CytC^[58b] that can also be linked to the dynamic intraglobular friction control in the same regime [manifested now through Eq. (9)]. Further analogy between the pressure and stabilizer dynamic effects comes from the “static” effect of the volume and compressibility decrease in both cases,^[57,58] as mentioned above. When going to thicker SAMs ($n = 4, 6, 11$), although the protein's internal viscosity (conformational flexibility that is coupled to CT) as such attains its slaving patterns unchanged, it becomes obscured and is no longer through Equations (6) and (9) owing to the drastic decrease in the electronic coupling parameter, H_{if} [see the “control” equation, Eq. (4)], and the onset of a nonadiabatic regime that now validates Equations (5) and (8). We also summarize the arguments exclusive of systematic changes in the pre-equilibrium factor (due to for example, the variable internal order of SAMs dis-

cussed in reference [73]) that may potentially interfere with our main results. Indeed, it is highly improbable that some variation of SAMs' internal order with the alkane length^[73] may cause significant changes in the pre-equilibrium term such as to exactly mimic three kinds of effects theoretically predictable *specifically* for the intrinsic CT constant. This argument, above all, is valid in the case of a “bulky” reactant, such as CytC reacting in the free regime at the solvent-separated distance from the SAM “surface”, presumably being almost insensitive to the extent of the SAM disorder (actually unimportant in most practical cases^[23–30,33]). In contrast, an attempt to ascribe our three kinetic relations (or one of these relations) favoring the mechanistic changeover to the variation in the pre-equilibrium term, unavoidably rises a cascade of rather awkward controversies; for example, the necessity to explain kinetic viscosity effects observed for CytC CT in “homogeneous”^[4b] and electrochemical regimes, the latter including tightly bound^[26,27,29] and freely diffusing^[32b] (also this work) cases by totally different inherent reasons, and so forth.

Conclusion

The gold disc electrodes coated with hydroxyl-terminated alkanethiol self-assembled monolayer films of variable thickness were used as versatile substrates for the CytC electron exchange. Due to the weak electrostatic interaction with the SAM ω -OH groups, CytC operates in a freely diffusing regime closely mimicking the molecular recognition pattern that subsists in living cells. Considering unbound CytC being the native (intact) species as a reference variant (ultimate alternative) for numerous irreversibly bound counterparts (probably heavily and diversely altered in a native structure), the impact of the electronic-coupling strength (gradually altered through the variation of the SAM thickness) on the CytC kinetic pattern in the freely diffusing regime has been systematically investigated for the first time. Also the impact of various important factors, such as high pressure up to 150 MPa (stabilizing CytC and directly altering the protein's internal friction), increased solution viscosity adjusted by addition of glucose (also stabilizing CytC and externally altering the protein's internal friction), and additives of the moderate denaturant urea, on the kinetic pattern of free CytC have been systematically investigated. For the first time the changeover of the sign of the activation volume has been detected for a given biochemical process, caused by the variation of a single intrinsic parameter, namely the electronic coupling strength.

Complementary to kinetic studies, for the cases of a glucose, urea, and pyridine additives of the same (or comparable) amounts, the thermodynamic stability pattern of free CytC has also been directly studied calorimetrically. The stabilizing route of glucose on CytC has been shown to have an essentially dual and cooperative nature, in which the second mechanism (slowly initiated but being much more effective) probably operates through the close protein–glu-

coarse interaction also responsible for a full kinetic (Kramers-type) viscosity effect (the latter suggested to be prognostic of dynamic slaving). The destabilizing route of urea on CytC indicated no sign of cooperative effects, exhibiting calorimetric behavior characteristic for the molten-globule-like species. No fraction of the native CytC has been detected either in urea or in pyridine-containing solutions by the DSC method. Surprisingly, the formal redox potential of CytC was only slightly altered on going to urea concentrations up to 6 M, and the 695 nm Met80-Fe^{III} CT band was still observable (although weakened) under these conditions, indicative of a survival of the native-like local protein folding. The decrease in the CytC heterogeneous CT rate constant in the case of the urea additives, unlike the case of a glucose viscosity effect (which is different for SAMs with $n=2, 3$ and $6, 11$, and attributable to the interplay of intrinsic CT mechanisms), is probably due to the weakening of CytC interaction with the SAM ω -OH groups (otherwise considered as softly attracting, allowing for the solvent-separated encounter complex).

In brief, the cross-testing of the CytC intrinsic ET mechanisms at the Au/SAM junctions (hydroxy-terminated n -alkanethiol SAMs), in the freely diffusing regime, through the variation of the SAM thickness ($n=2, 3, 4, 6, 11$), relative solution viscosity, $\eta_r=1$ to 4 (0.98 to 3.96 cP), and the hydrostatic pressure (up to 150 MPa), revealed a gradual turnover from the adiabatic to nonadiabatic regime with an intermediate mechanism found for $n=4$. The whole kinetic pattern can be reasonably well described within the unified theoretical model (extended CT theory). Our complex approach enabled the disclosure and profound analysis of the role of CT distance-dependent electronic coupling and of the protein's intrinsic viscosity (functionally important relaxational mobility). The diverse kinetic and thermodynamic impact of stabilizing/denaturing additives on both the kinetic and thermodynamic characteristics of CytC has also been studied and rationalized within the same theoretical framework invoking the concepts of the "molten-globule state" and "dynamic slaving".

Experimental Section

Materials: Horse heart CytC was purchased from Sigma Chemical Co (96% with a water content of 4%) and used either as received, by directly dissolving it in 500 mM Tris-HCl (Sigma), or 2 mM phosphate buffer (Sigma) containing 0.5 M KCl (Fluka), or after exhaustive ultra-filtration against the same buffer solutions. ω -Hydroxy alkanethiols [HO(CH₂) _{n} SH], $n=2, 3, 4, 6, 11$, used were 2-mercaptoethanol, 99% (Across), 3-mercapto-1-propanol, 95%, 4-mercapto-1-butanol, 95%, 6-mercapto-1-hexanol, 97%, 11-mercapto-1-undecanol, 97% (Aldrich). Other chemicals were decyltrimethylammonium bromide (Across), anhydrous glucose (Aldrich), urea (Across), and pyridine (Aldrich). Millipore MilliQ water was used throughout.

Gold disk electrodes of different diameter, 1.6 (BAS), 2, and 3 mm (Metrohm) were used as SAM-deposited substrates in bioelectrochemical kinetic experiments. They were treated according the procedures described elsewhere.^[25,33] In brief the electrode surface was cleaned with successive exposure to 60 °C sulfochromic acid and 5% HF. This procedure was re-

peated three times just before the immersion into 30 mM ω -hydroxy-alkanethiol solutions. The electrodes were kept in the coating solutions overnight to allow complete formation of SAM films.

Electrochemistry, high-pressure unit, and data processing: Electrochemical measurements (CV and steady-state) were carried out with an Autolab Electrochemical Analyzer PGSTAT30 (Eco-Chemie, The Netherlands) equipped with the General Purpose Electrochemical System (GPES) software for Windows (version 4.9). The pressure vessel and electrochemical cell were similar to those described earlier^[32a,49] with the difference that the working electrode was a 1.6 mm diameter gold disc electrode sealed in a Teflon cylinder (BAS). The working electrode, together with the auxiliary electrode (platinum wire) and the reference electrode (Ag/AgCl/4 M KCl) were sealed into the cell cap by two O-rings. The working volume of the HP electrochemical cell was 5 mL (see reference [30c] for more details). The assembled pressure vessel containing the cell was placed in a thermostated water jacket equilibrated at 25.0 ± 0.1 °C.

The working concentration of CytC was 5 to 10 mg mL⁻¹, that is, $(4-8) \times 10^{-4}$ M, throughout the electrochemical experiments. All the HP experiments were performed using a 500 mM Tris-HCl buffer at pH 7.4 (pH-meter reading for working solutions containing CytC). Tris buffer is known to withstand pressure induced pH changes.^[74] The same buffer was used in most of the other experiments in order to warrant comparable experimental conditions. A 2 mM phosphate buffer (plus 0.5 M KCl) of the same pH was also used in some cases for comparison purposes. Our calorimetric results (see Figure 5b in the Results and Discussion section) indicate that CytC in 500 mM Tris-HCl buffer is slightly less stable compared to the phosphate buffer. Yet it can definitely be considered to attain the native-like conformation (vide supra). A high ionic strength was necessary to exclude artifacts due to the uncompensated cell resistance.^[36] The latter was minimized (contribution to peak-to-peak separation less than 1%) as could be seen from the fact that the obtained kinetic constants in each case were essentially independent of the CV scan rate, electrode surface and CytC concentration in solution.

In cases where well-defined peak-shaped CV response was obtained (for $n=2$ to 6, see Figure 1a–c for the illustrative purpose), heterogeneous standard rate constants (i.e., the rate constants at zero overvoltage, that is, at zero driving force) and diffusion coefficients for electrodes modified by the ω -hydroxy alkanethiols [HO(CH₂) _{n} SH], $n=2, 3, 4, 6$, were calculated from the peak-to-peak separation and peak current values, respectively, according to well-established methodology^[34,35] (see also reference [32a] for more methodological details). The FSCV signal at $n=2$ to 6 in all cases displayed a shape typical for the reactant species operating in a freely diffusing regime^[23,25,32-36] (as opposed to the FSCV signal for the cases with strongly adsorbed CytC^[24,27,29]). In the case of a non-peak-shaped CV ($n=11$; Figure 1a), the rate constant was calculated by using data from the low overpotential region (initial portions of CV curves) in which the mass transport effect and other effects resulting in nonlinearity of the dependence of $\log(k_{\text{het}})$ on $\Delta E = E - E^0$ (Tafel plot) are negligible (see for example, reference [33] for details of the employed procedures). The concentrations of additives were as follows: glucose: 100, 200, 300, and 400 g L⁻¹ (0.56, 1.12, 1.67, and 2.24 M, respectively; in calorimetric experiments the highest glucose concentration was 600 g L⁻¹/3.36 M); urea: 2, 4, 6, and 8 M.

Optical spectra: The visible spectra (600 to 800 nm) of ferri-CytC solutions were recorded on a Hewlett Packard 8452 A Diode Array spectrophotometer. The solutions for these studies were essentially the same as for the electrochemical experiments.

Calorimetry and thermodynamic data processing: Differential scanning calorimetric experiments were performed on a Mettler Toledo DSC 822 instrument with a protein concentration of 55 mg mL⁻¹ (4.4 mM) in most cases. In few cases the protein concentration of 20 mg mL⁻¹ was applied in order to check possible impact of aggregation (vide infra). The samples (0.13 mL) containing 7.36 ± 0.04 mg protein were sealed in hermetic aluminum pans (0.15 mL). Buffer solutions with corresponding concentrations of additives were used in the reference pans. The temperature scan rate was 2 K min⁻¹ in all cases. The obtained heat flow W [J s⁻¹] signal was baseline corrected and transformed into the units of protein

excess heat capacity $C_p^{(\text{prot})}$ [$\text{J g}^{-1} \text{K}^{-1}$] by using Equation (12) (see, for example, reference [75]), in which v is the temperature scan rate [K s^{-1}] and m [g] is the protein weight in the sample solution.

$$C_p^{(\text{prot})} = \frac{W}{vm} \quad (12)$$

The calorimetric melting enthalpy was calculated according to Equation (13),^[11] in which T is the absolute temperature and T_1 and T_2 are the temperatures that correspond to the start and end of heat absorption due to thermal melting.^[39c]

$$\Delta H_{\text{cal}} = \int_{T_1}^{T_2} C_p^{(\text{prot})} dT \quad (13)$$

The control experiments with different protein concentrations yielded essentially same results, indicating relatively minor role of protein aggregation in the DSC performance. Importantly, under the standard conditions (no additives added) our calorimetric results reproduce most reliable literature data.^[7b,12b]

Acknowledgements

Resumption of the Alexander von Humboldt Fellowship for D.E.K. is kindly acknowledged. R.v.E. gratefully acknowledges financial support from the Deutsche Forschungsgemeinschaft as part of SFB 583 on "Redox-active Metal Complexes". D.E.K. is grateful to Prof. W. Schmickler for helpful comments.

- [1] a) G. W. Pettigrew, G. R. Moore, *Cytochromes C. Biological Aspects*, Springer, Berlin, **1987**; b) G. R. Moore, G. W. Pettigrew, *Cytochromes C. Evolutionary, Structural and Physicochemical Aspects*, Springer, Berlin, **1990**.
- [2] *Cytochrome C: A Multidisciplinary Approach* (Eds.: R. A. Scott, A. G. Mauk), University Science Books, Sausalito, CA, **1996**.
- [3] a) M. Ott, J. D. Robertson, V. Gogvadze, B. Zhivotovsky, S. Orrenius, *Proc. Natl. Acad. Sci. USA* **2002**, *99*, 1259–1263; b) Z. Hao, G. S. Duncan, C. C. Chang, A. Elia, M. Fang, A. Wakeham, H. Okada, T. Calzascia, Y. J. Jang, A. You-Ten, W.-C. Yeh, P. Ohashi, X. Wang, T. W. Mak, *Cell* **2005**, *121*, 579–591.
- [4] a) E. V. Pletneva, D. B. Fulton, T. Kohzuma, N. M. Kostic, *J. Am. Chem. Soc.* **2000**, *122*, 1034–1046; b) R. C. Lacey, L. Liu, L. Zang, M. Y. Ogawa, *Biochemistry* **2003**, *42*, 3904–3910.
- [5] a) M. Tetreault, S. H. Rongey, G. Feher, M. Y. Okamura, *Biochemistry* **2001**, *40*, 8452–8462; b) O. Miyashita, M. Y. Okamura, J. N. Onuchic, *Proc. Natl. Acad. Sci. USA* **2005**, *102*, 3558–3563.
- [6] a) P. Hildebrandt, M. Stockburger, *Biochemistry* **1989**, *28*, 6722–6728; b) P. Hildebrandt, *Biochim. Biophys. Acta* **1990**, *1040*, 175–186.
- [7] a) H. H. J. de Jongh, J. A. Killian, B. Kruijff, *Biochemistry* **1992**, *31*, 1636–1643; b) V. E. Bychkova, A. E. Dujsekina, S. I. Klenin, E. I. Tiktopulo, V. N. Uversky, O. B. Ptitsyn, *Biochemistry* **1996**, *35*, 6058–6063.
- [8] a) E. Sedlak, M. Antalík, J. Bagelova, M. Fedurco, *Biochim. Biophys. Acta* **1997**, *1319*, 258–266; b) M. Antalík, J. Bagelova, Z. Gazova, A. Musatov, D. Fedunova, *Biochim. Biophys. Acta* **2003**, *1646*, 11–20.
- [9] a) E. K. J. Tuominen, C. J. A. Wallace, P. K. J. Kinnunen, *J. Biol. Chem.* **2002**, *277*, 8822–8826; b) F. Daldal, M. Deshmukh, R. C. Prince, *Photosynth. Res.* **2003**, *76*, 127–134.
- [10] a) G. Cheddar, G. Tollin, *Arch. Biochem. Biophys.* **1994**, *310*, 392–396; b) E. J. Choi, E. K. Dimitriadis, *Biophys. J.* **2004**, *87*, 3234–3241.
- [11] a) P. L. Privalov, *Adv. Protein Chem.* **1979**, *33*, 167–241; b) P. L. Privalov, S. L. Gill, *Adv. Protein Chem.* **1988**, *39*, 191–234; c) P. L. Privalov, *J. Mol. Biol.* **1996**, *258*, 707–725.
- [12] a) M. Ohgushi, A. Wada, *FEBS Lett.* **1983**, *164*, 21–24; b) Y. Goto, S. Nishikiori, *J. Mol. Biol.* **1991**, *222*, 679–686; c) Y. Bai, S. W. Englander, *Proteins* **1996**, *24*, 145–151;
- [13] a) O. B. Ptitsyn, *J. Protein Chem.* **1987**, *6*, 273–293; b) O. B. Ptitsyn, *Curr. Opin. Struct. Biol.* **1995**, *5*, 74–78; c) O. B. Ptitsyn, in *Protein Folding* (Ed.: T. E. Creighton), Freeman, New York, **1993**, pp. 243–300; (d) V. N. Uversky, O. B. Ptitsyn, *J. Mol. Biol.* **1996**, *255*, 215–228.
- [14] a) N. Poklar, N. Petrovic, M. Oblak, G. Vesnaver, *Protein Sci.* **1999**, *8*, 832–840; b) D. E. Khoshtariya, M. Shushanyan, R. Sujashvili, M. Makharadze, E. Tabuashvili, G. Getashvili, *J. Biol. Phys. Chem.* **2003**, *3*, 2–10.
- [15] a) J. N. Onuchic, Z. Luthey-Schulten, P. G. Wolynes, *Annu. Rev. Phys. Chem.* **1997**, *48*, 545–600; b) C. L. Brooks, M. Gruebele, J. N. Onuchic, P. G. Wolynes, *Proc. Natl. Acad. Sci. USA* **1998**, *95*, 11037–11038.
- [16] a) H. Frauenfelder, P. W. Fenimore, B. H. McMahon, *Biophys. Chem.* **2002**, *98*, 35–48; b) P. W. Fenimore, H. Frauenfelder, B. H. McMahon, F. G. Parak, *Proc. Natl. Acad. Sci. USA* **2002**, *99*, 16047–16051; c) P. W. Fenimore, H. Frauenfelder, B. H. McMahon, R. D. Young, *Proc. Natl. Acad. Sci. USA* **2004**, *101*, 14408–14413.
- [17] a) A. M. Tsai, D. A. Neumann, L. N. Bell, *Biophys. J.* **2004**, *79*, 2728–2732; b) J. J. Hill, E. Y. Shalaev, G. Zografi, *J. Pharm. Sci.* **2005**, *94*, 1636–1667.
- [18] a) J. L. Green, J. Fan, C. A. Angell, *J. Phys. Chem.* **1994**, *98*, 13780–13790; b) C. A. Angell, *Science* **1995**, *267*, 1924–1935.
- [19] a) J. R. Winkler, H. B. Gray, *Chem. Rev.* **1992**, *92*, 369–379; b) H. B. Gray, J. R. Winkler, *Annu. Rev. Biochem.* **1996**, *65*, 537–561.
- [20] a) J. R. Winkler, A. J. Di Bilio, N. A. Farrow, J. H. Richards, H. B. Gray, *Pure Appl. Chem.* **1999**, *71*, 1753–1764; b) H. B. Gray, J. R. Winkler, *Proc. Natl. Acad. Sci. USA* **2005**, *102*, 3534–3539.
- [21] a) L. Qin, N. M. Kostić, *Biochemistry* **1994**, *33*, 12592–12599; b) M. M. Crnogorac, C. Shen, S. Young, Ö. Hansson, N. M. Kostić, *Biochemistry* **1996**, *35*, 16465–16474; c) M. M. Ivković-Jensen, G. M. Ullmann, S. Young, Ö. Hansson, M. M. Crnogorac, M. Ejdeback, N. M. Kostić, *Biochemistry* **1998**, *37*, 9557–9569.
- [22] a) M. Meier, J. Sun, J. F. Wishart, R. van Eldik, *Inorg. Chem.* **1996**, *35*, 1564–1570; b) J. Sun, C. Su, M. Meier, S. S. Isied, J. F. Wishart, R. van Eldik, *Inorg. Chem.* **1998**, *37*, 6129–6135.
- [23] a) M. Fedurco, *Coord. Chem. Rev.* **2000**, *209*, 263–331; b) M. Fedurco, J. Augustinski, C. Indiani, G. Smulevich, M. Antalík, M. Bano, E. Sedlak, M. C. Glascock, J. H. Dawson, *J. Am. Chem. Soc.* **2005**, *127*, 7638–7646.
- [24] a) M. J. Tarlov, E. F. Bowden, *J. Am. Chem. Soc.* **1991**, *113*, 1847–1849; b) S. Song, R. A. Clark, E. F. Bowden, M. J. Tarlov, *J. Phys. Chem.* **1993**, *97*, 6564–6569.
- [25] a) S. Terrettaz, J. Cheng, C. J. Miller, R. D. Guiles, *J. Am. Chem. Soc.* **1996**, *118*, 7857–7858; b) J. Cheng, S. Terrettaz, C. J. Blankman, C. J. Miller, R. D. Dangi, R. D. Guiles, *Isr. J. Chem.* **1997**, *37*, 259–266.
- [26] a) A. Avila, B. W. Gregory, K. Niki, T. M. Cotton, *J. Phys. Chem. B* **2000**, *104*, 2759–2766; b) K. Niki, W. R. Hardi, M. G. Hill, H. Li, J. R. Sprinkle, E. Margoliash, K. Fujita, R. Tanimura, N. Nakamura, H. Ohno, J. H. Richards, H. B. Gray, *J. Phys. Chem. B* **2003**, *107*, 9947–9949.
- [27] a) H. Yamamoto, H. Liu, D. H. Waldeck, *Chem. Commun.* **2001**, 1032–1033; b) J. Wei, H. Liu, A. R. Dick, H. Yamamoto, Y. He, D. H. Waldeck, *J. Am. Chem. Soc.* **2003**, *125*, 7704–7714.
- [28] a) H. D. Sikes, J. F. Smalley, S. P. Dudek, A. R. Cook, M. D. Newton, C. E. D. Chidsey, S. W. Feldberg, *Science* **2001**, *291*, 1519–1523; b) J. F. Smalley, H. O. Finklea, C. E. D. Chidsey, M. R. Linford, S. E. Creager, J. P. Ferraris, K. Chalfant, T. Zawodzinski, S. W. Feldberg, M. D. Newton, *J. Am. Chem. Soc.* **2003**, *125*, 2004–2013.

- [29] a) J. Wei, H. Liu, D. E. Khoshitariya, H. Yamamoto, A. Dick, D. H. Waldeck, *Angew. Chem.* **2002**, *114*, 4894–4897; *Angew. Chem. Int. Ed.* **2002**, *41*, 4700–4703; b) D. E. Khoshitariya, J. Wei, H. Liu, H. Yue, D. H. Waldeck, *J. Am. Chem. Soc.* **2003**, *125*, 7704–7714.
- [30] a) D. H. Murgida, P. Hildebrandt, *J. Am. Chem. Soc.* **2001**, *123*, 4062–4068; b) D. H. Murgida, P. Hildebrandt, *Acc. Chem. Res.* **2004**, *37*, 854–861; c) D. H. Murgida, P. Hildebrandt, *Phys. Chem. Chem. Phys.* **2005**, *7*, 3773–3784.
- [31] a) K. Ataka, J. Heberle, *J. Am. Chem. Soc.* **2003**, *125*, 4986–4987; b) K. Ataka, J. Heberle, *J. Am. Chem. Soc.* **2004**, *126*, 9445–9457.
- [32] a) T. D. Dolidze, D. E. Khoshitariya, D. H. Waldeck, J. Macyk, R. van Eldik, *J. Phys. Chem. B* **2003**, *107*, 7172–7179; b) D. E. Khoshitariya, T. D. Dolidze, D. Sarauli, R. van Eldik, *Angew. Chem.* **2006**, *118*, 283–287; *Angew. Chem. Int. Ed.* **2006**, *45*, 277–281.
- [33] a) D. E. Khoshitariya, T. D. Dolidze, L. D. Zusman, D. H. Waldeck, *J. Phys. Chem. A* **2001**, *105*, 1818–1829; b) C. J. Miller, P. Cuendet, M. Grätzel, *J. Phys. Chem.* **1991**, *95*, 877–886.
- [34] a) R. S. Nicholson, *Anal. Chem.* **1965**, *37*, 1351–1355; b) R. S. Nicholson, I. Shain, *Anal. Chem.* **1964**, *36*, 706–723.
- [35] A. J. Bard, L. R. Faulkner, *Electrochemical Methods. Fundamentals and Applications*, 2nd ed., Wiley, New York, **2001**, pp. 226–260.
- [36] a) F. A. Armstrong, H. A. Hill, N. J. Walton, *Acc. Chem. Res.* **1988**, *21*, 407–413; b) A. M. Bond, *Inorg. Chim. Acta* **1994**, *226*, 293–340.
- [37] a) M. D. Newton, H. L. Friedman, *J. Chem. Phys.* **1985**, *83*, 5210–5218; b) J. T. Hupp, M. J. Weaver, *J. Electroanal. Chem. Interfacial Electrochem.* **1983**, *152*, 1–14; c) A. Gochev, G. E. McManis, M. J. Weaver, *J. Chem. Phys.* **1989**, *91*, 906–916.
- [38] a) L. D. Zusman, *Chem. Phys.* **1980**, *49*, 295–304; b) L. D. Zusman, *Chem. Phys.* **1987**, *112*, 53–59; c) L. D. Zusman, *Z. Phys. Chem.* **1994**, *186*, 1–29.
- [39] a) D. F. Calef, P. G. Wolynes, *J. Phys. Chem.* **1983**, *87*, 3387–3400; b) J. T. Hynes, *J. Phys. Chem.* **1986**, *90*, 3701–3706; c) W. Schmickler, J. Mohr, *J. Chem. Phys.* **2002**, *117*, 2867–2872.
- [40] a) D. N. Beratan, J. N. Onuchic, *J. Chem. Phys.* **1988**, *89*, 6195–6203; b) M. Bixon, J. Jortner, *Adv. Chem. Phys.* **1999**, *106*, 35–202; c) R. Kosloff, M. A. Ratner, *J. Phys. Chem. B* **2002**, *106*, 8479–8483.
- [41] a) R. R. Dogonadze, A. M. Kuznetsov, *Prog. Surf. Sci.* **1975**, *6*, 1–41; b) R. R. Dogonadze, A. M. Kuznetsov, J. Ulstrup, *J. Theor. Biol.* **1977**, *69*, 239–263.
- [42] a) R. A. Marcus, N. Sutin, *Biochim. Biophys. Acta* **1985**, *811*, 265–322; b) D. N. Beratan, J. N. Betts, J. N. Onuchic, *Science* **1991**, *252*, 1286–1288.
- [43] H. A. Kramers, *Physica* **1940**, *7*, 284–304.
- [44] D. Beece, L. Eisenstein, H. Frauenfelder, D. Good, M. C. Marden, L. Reinish, A. H. Reynolds, L. B. Sorensen, K. T. Yue, *Biochemistry* **1980**, *19*, 5147–5157.
- [45] a) D. E. Khoshitariya, *Biofizika* **1986**, *31*, 391–394; b) N. G. Gogvadze, D. E. Khoshitariya, J. M. Hammerstad-Pedersen, J. Ulstrup, *Eur. J. Biochem.* **1991**, *200*, 423–429.
- [46] B. Gavish, S. Yedgar, in *Protein–Solvent Interactions* (Ed.: R. B. Gregory), Marcel Dekker, New York, **1995**, pp. 343–373.
- [47] a) *Inorganic High-Pressure Chemistry. Kinetics and Mechanisms* (Ed.: R. van Eldik), Elsevier, Amsterdam, **1986**; b) *High Pressure Chemistry* (Eds.: R. van Eldik, F.-G. Klärner), Wiley-VCH, Weinheim, **2002**.
- [48] a) R. van Eldik, T. Asano, W. J. Le Noble, *Chem. Rev.* **1989**, *89*, 549–688; b) A. Drljaca, C. D. Hubbard, R. van Eldik, T. Asano, M. V. Basilevsky, W. J. Le Noble, *Chem. Rev.* **1998**, *98*, 2167–2290.
- [49] a) Y. Fu, A. S. Cole, T. W. Swaddle, *J. Am. Chem. Soc.* **1999**, *121*, 10410–10415; b) T. W. Swaddle, P. A. Tregloan, *Coord. Chem. Rev.* **1999**, *187*, 255–289; c) T. W. Swaddle, *Chem. Rev.* **2005**, *105*, 2573–2608.
- [50] a) N. A. Lewis, Y. S. Obeng, D. V. Taveras, R. van Eldik, *J. Am. Chem. Soc.* **1989**, *111*, 924–927; b) N. A. Lewis, R. R. McNeer, D. V. Taveras, *Inorg. Chim. Acta* **1994**, *225*, 89–93; c) D. E. Khoshitariya, R. Billing, M. Ackermann, R. van Eldik, *J. Chem. Soc. Faraday Trans.* **1995**, *91*, 1625–1629.
- [51] a) O. Miyashita, N. Go, *J. Phys. Chem. B* **1999**, *103*, 562–571; b) V. Furukawa, K. Ishimori, I. Moroshima, *J. Phys. Chem. B* **2000**, *104*, 1817–1825.
- [52] a) Y. I. Kharkats, L. I. Krishtalik, *J. Theor. Biol.* **1985**, *112*, 221–249; b) I. Muegge, P. X. Qi, A. J. Wand, Z. T. Chu, A. Warshel, *J. Phys. Chem. B* **1997**, *101*, 825–836.
- [53] Y.-P. Liu, M. D. Newton, *J. Phys. Chem.* **1994**, *98*, 7162–7169.
- [54] a) B. M. Hoffman, M. A. Ratner, *J. Am. Chem. Soc.* **1987**, *109*, 6237–6243; b) V. Davidson, *Acc. Chem. Res.* **2000**, *33*, 87–93; c) An important role of the adiabatic (friction controlled) mechanism for liquid-phase biological CT processes is extensively discussed in papers by Cherepanov et al. and Kotelnikov et al. in reference [55].
- [55] a) D. A. Cherepanov, L. I. Krishtalik, A. Y. Mulikdjanian, *Biophys. J.* **2001**, *80*, 1033–1049; b) A. I. Kotelnikov, J. M. Ortega, E. S. Medvedev, B. L. Psikha, D. Garcia, P. Mathis, *Bioelectrochemistry* **2002**, *56*, 3–8.
- [56] Although Ataka and Heberle^[31b] reported adsorption of CytC on ω -OH SAMs, in our case this is excluded due to sufficiently high ionic strength, also visualized by the CV specification (see Experimental Section).
- [57] a) P. Cioni, G. B. Strambini, *J. Mol. Biol.* **1994**, *242*, 291–301; b) A. Prieu, A. Almagor, S. Yedgar, B. Gavish, *Biochemistry* **1996**, *35*, 2061–2066.
- [58] a) N. Taulier, T. V. Chalikian, *Biochim. Biophys. Acta* **2002**, *1595*, 48–70; b) D. N. Dubins, R. Filfil, R. B. Macgregor, T. V. Chalikian, *Biochemistry* **2003**, *42*, 8671–8678.
- [59] R. Ravindra, R. Winter, *ChemPhysChem* **2004**, *5*, 566–571.
- [60] a) T. Pineda, J. M. Sevilla, A. J. Roman, M. Blazquez, *Biochim. Biophys. Acta* **1997**, *1343*, 227–234; b) A. A. Moosavi-Movahedi, J. Chamani, H. Chourchian, H. Shafiey, C. M. Sorenson, N. Sheibani, *J. Protein Chem.* **2003**, *22*, 23–30.
- [61] a) B. A. Feinberg, X. Liu, M. D. Ryan, A. Schejter, C. Zhang, E. Margoliash, *Biochemistry* **1998**, *37*, 13091–13101; b) C. Fan, B. Gillespie, G. Wang, A. J. Heeger, K. W. Plaxco, *J. Phys. Chem. B* **2002**, *106*, 11375–11383.
- [62] a) R. Santucci, C. Bongiovanni, G. Mei, T. Ferri, F. Polizio, A. Desideri, *Biochemistry* **2000**, *39*, 126–32–12638; b) Y.-S. Kim, L. S. Jones, A. Dong, B. S. Kendrick, B. S. Chang, M. C. Manning, T. W. Randolph, J. F. Carpenter, *Protein Sci.* **2003**, *12*, 1252–1261.
- [63] a) B. S. Russel, R. Melenkivitz, K. L. Bren, *Proc. Natl. Acad. Sci. USA* **2000**, *97*, 8312–8317; b) M. Fedurco, J. Augustinski, C. Indiani, G. Smulevich, M. Antalík, M. Bano, E. Sedlak, M. C. Glascock, J. H. Dawson, *Biochim. Biophys. Acta* **2004**, *1703*, 31–41.
- [64] K. Kawahara, C. Tanford, *J. Biol. Chem.* **1966**, *241*, 3228–3232.
- [65] a) D. E. Khoshitariya, T. D. Dolidze, P. Lindqvist-Reis, A. Neubrand, R. van Eldik, *J. Mol. Liq.* **2002**, *96/97*, 45–63; b) D. E. Khoshitariya, A. Zahl, T. D. Dolidze, Neubrand, R. van Eldik, *ChemPhysChem* **2004**, *5*, 1398–1404.
- [66] a) N. Agmon, *J. Phys. Chem.* **1996**, *100*, 1072–1080; b) A. Geiger, M. Kleene, D. Paschek, A. Rehtanz, *J. Mol. Liq.* **2003**, *106*, 131–146.
- [67] a) P. J. Artimiuk, C. C. T. Blake, D. E. P. Grace, S. J. Oatley, D. C. Phillips, M. J. E. Sternberg, *Nature* **1979**, *280*, 563–568; b) P. Zavadzky, J. Kardos, A. Svingor, G. A. Petsko, *Proc. Natl. Acad. Sci. USA* **1998**, *95*, 7406–7411; c) D. Vitkup, D. Ringe, G. A. Petsko, M. Karplus, *Nat. Struct. Biol.* **2000**, *7*, 34–38.
- [68] a) A. Ansari, C. M. Jones, E. R. Henry, J. Hofrichter, W. A. Eaton, *Biochemistry* **1994**, *33*, 5128–5145; b) D. Sagnella, J. E. Straub, D. Thirumalai, *J. Chem. Phys.* **2000**, *113*, 7702–7711.
- [69] a) K. Heremans, L. Smeller, *Biochim. Biophys. Acta* **1998**, *1386*, 353–370; b) K. Heremans, L. Smeller, in *Biological Systems under Extreme Conditions* (Eds.: Y. Taniguchi, H. E. Stanley, H. Ludwig), Springer, Berlin, Heidelberg, **2002**, pp. 53–73.
- [70] H. Frauenfelder, N. A. Alberding, A. Ansari, D. Braunstein, B. Cowen, M. K. Hong, I. E. T. Iben, J. B. Johnson, S. Luck, M. C. Marden, J. R. Mourant, P. Ormos, L. Reinisch, R. Scholl, A. Schulte, E. Shyamsunder, L. B. Soremen, P. J. Steinbach, A. Xie, R. D. Young, K. T. Yue, *J. Phys. Chem.* **1990**, *94*, 1024–1037.

- [71] a) R. D. Lins, C. S. Pereira, P. H. Hünenberger, *Protein J.* **2004**, *33*, 177–186; b) In this work and in reference [59] much higher concentrations of sugars are considered both theoretically and experimentally as compared to the more traditional approach formulated in reference [72].
- [72] a) S. N. Timasheff, *Proc. Natl. Acad. Sci. USA* **2002**, *99*, 14408–14413; b) S. N. Timasheff, *Biochemistry* **2002**, *41*, 13473–13482.
- [73] a) M. D. Porter, T. B. Bright, D. L. Allara, C. E. D. Chidsey, *J. Am. Chem. Soc.* **1987**, *109*, 3559–3568; b) V. Bindu, T. Pradeep, *Vacuum* **1998**, *49*, 63–66; c) N. Sandhyarani, T. Pradeep, *Int. Rev. Phys. Chem.* **2003**, *22*, 221–262.
- [74] a) R. C. Newmann, W. Kauzmann, A. Zipp, *J. Phys. Chem.* **1973**, *77*, 2687–2691; b) Y. Kitamura, T. Itoh, *J. Solution Chem.* **1987**, *16*, 715–725.
- [75] a) B. Wunderlich, Y. Jin, A. Boller, *Thermochim. Acta* **1994**, *238*, 277–293; b) M. Reading, A. Luget, R. Wilson, *Thermochim. Acta* **1994**, *238*, 295–307; c) However, the reported values are given in more traditional units of kilocalories (1 cal = 4.148 J).

Received: January 16, 2006

Revised: May 17, 2006

Published online: August 3, 2006